Seelig, J., Tamm, L., Hymel, L., & Fleischer, S. (1981) *Biochemistry 20*, 3922–3933.
Seeman, P. (1972) *Pharmacol. Rev. 24*, 583–655.
Siminovitch, D. J., Rance, M., & Jeffrey, K. R. (1980) *FEBS Lett. 112*, 79–82.
Singer, M. A., & Jain, M. K. (1980) *Can. J. Biochem. 58*, 815–821.
Singleton, W. S., Gray, M. S., Brown, M. L., & White, J. L. (1965) *J. Am. Oil Chem. Soc. 42*, 53–56.
Sixl, F., & Watts, A. (1982) *Biochemistry 21*, 6446–6452.
Sixl, F., Brophy, P. J., & Watts, A. (1984) *Biochemistry 23*, 2032–2039.
Tamm, L. K., & Seelig, J. (1983) *Biochemistry 22*, 1474–1483.
Taylor, M. G., & Smith, I. C. P. (1980) *Biochim. Biophys. Acta 599*, 140–149.
Taylor, M. G., & Smith, I. C. P. (1981a) *Chem. Phys. Lipids 28*, 119–136.
Taylor, M. G., & Smith, I. C. P. (1981b) *Biochemistry 20*, 5252–5255.
Thayer, A. M., & Kohler, S. J. (1981) *Biochemistry 20*, 6831–6834.
Westman, J., Boulanger, Y., Ehrenberg, A., & Smith, I. C. P. (1982) *Biochim. Biophys. Acta 685*, 315–328.

^{19}F NMR Investigation of Molecular Motion and Packing in Sonicated Phospholipid Vesicles†

Wen-Guey Wu, Susan R. Dowd, Virgil Simplaceanu, Zheng-Yu Peng, and Chien Ho*
Department of Biological Sciences, Carnegie-Mellon University, Pittsburgh, Pennsylvania 15213
Received March 14, 1985

ABSTRACT: Dimyristoylphosphatidylcholine (DMPC) labeled with a $C^{19}F_2$ group in the 4-, 8-, or 12-position of the 2-acyl chain has been investigated in sonicated unilamellar vesicles (SUV) by fluorine-19 nuclear magnetic resonance (NMR) at 282.4 MHz from 26 to 42 °C. The ^{19}F NMR spectra exhibit two overlapping resonances with different line widths. Spin–lattice relaxation time measurements have been performed in both the laboratory frame (T_1) and the rotating frame ($T_{1\rho}$) in order to investigate the packing and dynamics of phospholipids in lipid bilayers. Quantitative line-shape and relaxation analyses are possible by using the experimental chemical shift anisotropy ($\Delta\nu_{CSA}$) and the internuclear F–F vector order parameter (S_{FF}) values obtained from the ^{19}F powder spectra of multilamellar liposomes. The following conclusions can be made: (i) The ^{19}F chemical shift difference between the inside and outside leaflets of SUV can be used to monitor the lateral packing of the phospholipid in the two SUV monolayers. The hydrocarbon chains in the outer layer are found to be more tightly packed than those of the inner one, and the differences between them become smaller near the chain terminals. (ii) The effective correlation time [$(1–4) \times 10^{-7}$ s] obtained from either the motional narrowing of the line widths or off-resonance $T_{1\rho}$ measurements is shorter than that estimated from the Stokes–Einstein diffusion model (10^{-6} s), on the basis of a hydrodynamic radius of 110 Å for SUV. (iii) $T_{1\rho}$, but not T_1, is found to be different for the inside and outside resonances of the SUV, indicating that slower motions (10^{-7} s) are responsible for the different line widths of the two resonances. (iv) The Arrhenius activation energies determined from T_1 values for the 4- and 8-^{19}F-labeled positions (5 kJ/mol) are lower than those obtained for the 12-position (10 kJ/mol). ^1H T_1 measurements on both the ^{19}F-labeled and unlabeled sonicated DMPC vesicles indicate that there is no perturbation of the fatty acyl chain packing by the CF_2 group. (v) The curvature in the SUV perturbs the fatty acyl chain packing mainly in the outside leaflet of the bilayer.

Fluorine-19 has recently received attention as an attractive nuclear magnetic resonance (NMR)[1] probe for membrane studies [for a recent review, see Ho et al. (1985)]. To investigate lipid fatty acyl chain order and dynamics in both model and biological membranes, myristoyl([$^{19}F_2$]difluoromyristoyl)phosphatidylcholine ([$^{19}F_2$]DMPC) has been used as a sensitive probe. By applying various NMR techniques such as the Carr–Purcell–Meiboom–Gill multiple-pulse sequence (Post et al., 1984) and line-shape analysis (Engelsberg et al., 1982; Dowd et al., 1984) to both oriented multilayers and random multilamellar liposomes of [$^{19}F_2$]DMPCs, this laboratory has determined the order parameter, S_{FF}, for the F–F internuclear vector from the Pake doublet splitting. In addition, it has become clear that, at high magnetic fields (7

† This paper was presented in part at the 8th International Biophysics Congress, July 27 to Aug 3, 1984, in Bristol, England. This work was supported by research grants from the National Science Foundation (DMB 82-08829) and the National Institutes of Health (GM-26874 and HL-24525).
* Author to whom correspondence should be addressed.

[1] Abbreviations: NMR, nuclear magnetic resonance; DMPC, dimyristoylphosphatidylcholine; [$^{19}F_2$]DMPC, myristoyl([$^{19}F_2$]difluoromyristoyl)phosphatidylcholine; 2-[4,4-$^{19}F_2$]DMPC, 1-myristoyl-2-(4,4-[$^{19}F_2$]difluoromyristoyl)-*sn*-glycero-3-phosphocholine; 2-[8,8-$^{19}F_2$]-DMPC, 1-myristoyl-2-(8,8-[$^{19}F_2$]difluoromyristoyl)-*sn*-glycero-3-phosphocholine; 2-[12,12-$^{19}F_2$]DMPC, 1-myristoyl-2-(12,12-[$^{19}F_2$]difluoromyristoyl)-*sn*-glycero-3-phosphocholine; EDTA, ethylenediaminetetraacetic acid; Tris, tris(hydroxymethyl)aminomethane; TFA, trifluoroacetic acid; S_{FF}, the internuclear fluorine–fluorine vector order parameter; CSA, chemical shift anisotropy; SUV, sonicated unilamellar vesicle(s); T_1, spin–lattice relaxation time in the laboratory frame; $T_{1\rho}$, spin–lattice relaxation time in the rotating frame; T_2, spin–spin relaxation time; T_2^*, apparent spin–spin relaxation time; M_L, steady-state value of the magnetization component aligned with the main magnetic field; M_{eff}, steady-state value of the magnetization component aligned with the effective magnetic field in the presence of the off-resonance field.

0006-2960/85/0424-7153$01.50/0

T), the chemical shift anisotropy (CSA) dominates the ^{19}F NMR line shape. From our interpretation of the ^{19}F NMR spectrum obtained for multilamellar liposomes, we have been able to extend our investigation to an analysis of sonicated unilamellar vesicles (SUV).

The difficulty in resolving the overlapping resonances arising from fatty acyl methylene groups in both ^1H and ^2H NMR studies of SUV has given rise to a controversy over the NMR line-shape analysis and the presence of motional differences in the acyl chains between SUV and multilayers (Stockton et al., 1976; Bloom et al., 1978; Parmar et al., 1984). Both the ^{19}F NMR (Longmuir & Dahlquist, 1976) and the 500-MHz ^1H NMR spectra (Schuh et al., 1982) of vesicles show chemical shift nonequivalence and resonance line-width differences between the acyl chains located in the inside and outside leaflets. Despite the overlapping resonances from various fatty acyl methylene protons in the ^1H NMR, the line width of the inside resonance can be seen to be approximately one-third of the outside resonance. These observations would indicate that ^2H NMR spectra of various selectively deuterated lipids should not be analyzed as a single resonance (Stockton et al., 1976; Parmar et al., 1984). Our present ^{19}F NMR study of SUV allows us to address the problems of phospholipid packing and dynamics more directly.

In addition to an analysis of the motional narrowing of the ^{19}F NMR line width, the result of an alternative technique for measuring intermediate slow motion, i.e., spin–lattice relaxation in the rotating frame ($T_{1\rho}$), is detailed here. Since the anisotropic chemical shift is expected to dominate the ^{19}F relaxation mechanism (see Theory), the present work will also emphasize an analysis of lipid bilayer dynamics using the chemical shift anisotropy (CSA). By combining information obtained from the chemical shift and the relaxation studies, ^{19}F NMR investigations offer a unique method for studying the molecular order and motions of phospholipids in model membranes.

Experimental Procedures

Materials. 1-Myristoyl-2-(4,4-[$^{19}F_2$]difluoromyristoyl)-*sn*-glycero-3-phosphocholine (2-[4,4-$^{19}F_2$]DMPC) and the corresponding 8,8-[$^{19}F_2$]difluoro (2-[8,8-$^{19}F_2$]DMPC) and 12,12-[$^{19}F_2$]difluoro (2-[12,12-$^{19}F_2$]DMPC) derivatives were synthesized by methods equivalent to those described previously for the preparation of 2-[8,8-$^{19}F_2$]DMPC (Engelsberg et al., 1982). ^1H NMR spectra of the phospholipids taken in deuteriochloroform solutions were consistent with the expected structures. Deuterium oxide was purchased from Bio-Rad. Sepharose CL-4B was obtained from Sigma. Reagent-grade solvents were used unless otherwise stated.

Preparation of SUV. Small, single-walled vesicles, homogeneous in size, were prepared by a modification of Huang's (1969) procedure. ^{19}F-Labeled lipid dispersions in a standard buffer solution (50 mM Tris, 100 mM NaCl, 1 mM EDTA, pH 7.4) were sonicated with a Branson probe-type sonicator. Sonication of the dispersions was carried out above the phase transition temperature, 2-[8,8-$^{19}F_2$]DMPC and 2-[12,12-$^{19}F_2$]DMPC at 22 °C and 2-[4,4-$^{19}F_2$]DMPC at 35 °C. High-speed centrifugation at 50 000 rpm (Barenholz et al., 1977) of the sonicate gave homogeneous dispersions as a clear band at the top. The vesicles used for the spin–lattice relaxation time (T_1) measurements were additionally dialyzed against D_2O solution to decrease the ^1H signal of H_2O.

NMR Measurements. NMR spectra were obtained on a Bruker WH-300 wide-bore spectrometer equipped with an Aspect 2000A computer, operating in the Fourier-transform mode, using standard as well as home-made devices and experimental set-ups. In all cases, the temperature was stabilized to ±0.5 °C.

^1H NMR spectra of the sonicated unilamellar vesicles (SUV) were obtained at 300 MHz, in 10% D_2O (for field lock) buffer solution, with the following parameters: a 16-bit digitizer, spectral widths from 1500 to 4000 Hz, 8K points, averaging typically 128 transients, and 75° pulses of 5 μs, repeated every 3–4.5 s. The main water signal was diminished by gated irradiation with the decoupler. ^1H T_1 measurements were done by inversion–recovery in 99% D_2O buffer solution, with no water suppression employed.

^{19}F NMR spectra of the vesicles were obtained at 282.4 MHz with a Bruker high-resolution 5-mm ^{19}F probe. For the measurement of the temperature dependence of the chemical shifts, the spectra are referenced to an internal 2-mm capillary containing 10 mM trifluoroacetic acid (TFA) in H_2O. Negative chemical shifts are upfield from the reference signal. No proton decoupling was used. In general, 200 scans were averaged at each temperature for 2-[12,12-$^{19}F_2$]DMPC and 2-[8,8-$^{19}F_2$]DMPC, while 800 scans were needed for the 2-[4,4-$^{19}F_2$]DMPC vesicles. A spectral width of 12 200 Hz, an acquisition time of 0.34 s (size 8K), a relaxation delay of 1 s, and 75° pulse of 5 μs were used. The analysis of the line shapes was performed on a VAX 11/780 computer by fitting to a pair of Lorentzian lines, so as to determine individual line widths and positions of the inner and outer leaflet resonances.

^{19}F T_1 measurements were carried out by inversion–recovery with a standard 5-mm probe head with no proton irradiation. Generally, 256 scans were averaged for each of the 11 delays spanning 4 T_1 or more. The recovery curves were exponential and were processed with the Bruker DISNMR software using a T_1 nonlinear fitting routine.

Off-resonance $T_{1\rho}$ measurements were carried out in a manner similar to that of James et al. (1977), using a home-built 5-mm multiarray solenoidal coil (Cook & Lowe, 1982; Engelsberg et al., 1982). The Bruker spectrometer was rewired and supplemented with a homemade transmitter, able to deliver radio-frequency pulses having different amplitudes and arbitrary lengths, within the same pulse sequence. M_{eff} was measured with the pulse sequence $[(D_1\text{–}PW_1\text{–}D_2)\text{–}PW_2\text{–}AQ]_n$ with D_1 of 3.0 s, PW_1 ($\sim 6T_1$) of 2.4 s, D_2 ($\sim 3T_2^*$) of 23 ms, and PW_2 (90°) of 5.8 μs. M_L was determined from the sequence $(D_1\text{–}PW_2\text{–}AQ)_n$. The amplitude of the off-resonance radio-frequency field pulse PW_1 was 1 G (4 kHz), while the 90° measuring pulse PW_2 (in resonance) was 10.7 G (42.9 kHz). The measuring pulse was preceded by a 23-ms ($\sim 3T_2^*$) delay, D_2, in order to allow all the transverse magnetization created during the locking pulse to decay. The short T_2 (compared to T_1) made a homospoil pulse unnecessary.

Theory

^{19}F NMR Line-Shape Analysis of Multilamellar Liposomes. The ^{19}F NMR powder pattern line shapes observed for the C$^{19}F_2$-labeled phospholipid dispersions can be understood on the basis of dipolar interactions (homonuclear, $\Delta\nu_{FF}$; heteronuclear, $\Delta\nu_{FH}$) and an anisotropic ^{19}F chemical shift ($\Delta\nu_{CSA}$) [for example, see Ho et al. (1985)]. A mathematical procedure to de-Pake the NMR powder spectrum has been used to extract the spectral information (i.e., $\Delta\nu_{FF}$, $\Delta\nu_{FH}$, and $\Delta\nu_{CSA}$) needed for our line-shape and relaxation analyses (Bloom et al., 1981). Details of the procedure can be found in Dowd et al. (1984). Table I lists one set of data for three different ^{19}F-labeled lipid dispersions at 27 °C. At a magnetic field strength of 7 T, it can be seen that the magnitude of $\Delta\nu_{CSA}$ is much larger than that of the dipole–dipole interac-

Table I: ^{19}F Chemical Shift Anisotropy ($\Delta\nu_{CSA}$), Homonuclear Dipolar Interaction ($\Delta\nu_{FF}$), and Heteronuclear Dipolar Interaction ($\Delta\nu_{FH}$) for Three Different ^{19}F-Labeled Lipids in Multilamellar Dispersions at 27 °C and at a Magnetic Field Strength of 7 T

probe	$\Delta\nu_{CSA}$ (kHz)	$\Delta\nu_{FF}$ (kHz)	$\Delta\nu_{FH}$ (kHz)
2-[4,4-$^{19}F_2$]DMPC	19.7	3.2	1.5
2-[8,8-$^{19}F_2$]DMPC	16.3	2.8	1.3
2-[12,12-$^{19}F_2$]DMPC	9.9	1.8	0.8

tions, $\Delta\nu_{FF}$ and $\Delta\nu_{FH}$. Also of interest is the fact that the CSA correlates linearly with the order parameter, S_{FF} (Dowd et al., 1984).

Motional Narrowing of ^{19}F NMR Spectra of Sonicated Vesicles. ^{19}F NMR spectra of SUV differ dramatically from those of lamellae. Instead of axially symmetric powder spectra, two overlapping Lorentzian resonances with different line widths are observed (Longmuir & Dahlquist, 1976). It has been suggested by ^{1}H and ^{2}H NMR studies that the narrow lines result from averaging of the powder spectra by either isotropic reorientation of the spherical vesicles (Stockton et al., 1976; Bloom et al., 1978) or additional motion of the phospholipid molecules caused by the highly curved surface of the vesicles (Bocian & Chan, 1978; Parmar et al., 1984). To relate the ^{19}F NMR spectra of SUV and of multilamellar dispersions, we define a correlation time, τ_v, describing the tumbling of the entire vesicle in the solution and diffusion of the lipids around the surface of the vesicle with correlation times, τ_r and τ_d (Bloom et al., 1975):

$$\tau_v^{-1} = \tau_r^{-1} + \tau_d^{-1} \quad (1)$$

From the hydrodynamic radius (R = 110 Å) of SUV (Huang & Mason, 1978) and the lateral diffusion coefficient for phospholipids ($D = 10^{-8}$ cm^2/s) (Wu & Huang, 1981), the effective correlation time can be found to be about 10^{-6} s at 27 °C, on the basis of the Stokes–Einstein diffusion model (Stockton et al., 1976). Although this motion is slow in terms of the ^{19}F NMR frequency (282.4 MHz), it can be considered as fast compared to the residual width of ^{19}F spectra of multilamellar liposomes, i.e., $2\pi\Delta\nu_{CSA}\tau_v \ll 1$ (Table I). It is, thus, possible to use the two-step application of classical relaxation theory to the rapid local motion of fatty acyl chains and the slower overall motion of the vesicle [for details, see Stockton et al. (1976)].

Since, as in previous ^{1}H relaxation measurement studies (Kroon et al., 1976), the contribution of $\Delta\nu_{FH}$ was observed to be relatively small, it will be considered as negligible. The theoretical aspects of the dipole–dipole interaction through like spins, such as geminal protons in the methylene group, have been treated quite extensively by other studies (Bloom et al., 1978; Pace & Chan, 1982). To avoid redundancy, we will present our analysis on the basis of the CSA relaxation mechanism. The dipolar contribution of the geminal fluorines will be shown to be much smaller than the CSA contribution.

Quantitatively, the CSA contribution to the total relaxation rate may be estimated according to [cf. p 316 of Abragam (1961) and the Appendix]

$$T_1^{-1} = (2/15)\omega_0^2\delta^2 J(\omega_0) \quad (2)$$

$$T_2^{-1} = (1/90)\omega_0^2\delta^2[3J(\omega_0) + 4J(0)] \quad (3)$$

$$T_{1\rho}^{-1} = (2/45)\omega_0^2\delta^2[(\sin^2\theta)J(\omega_e) + (3/2) \times [\sin^4(\theta/2)]J(\omega_0 - \omega_e) + (3/2)[\cos^4(\theta/2)]J(\omega_0 + \omega_e)] \quad (4)$$

where the spectral density $J(\omega)$ is given as

$$J(\omega) = 2\tau_c/(1 + \omega^2\tau_c^2) \quad (5)$$

Equations 2–4 are strictly valid only for an isotropic motion characterized by a single correlation time, τ_c, with an axially symmetric chemical shift anisotropy, δ (ppm) = $2\pi\Delta\nu_{CSA}/\omega_0$. For the ^{19}F nuclei frequency used (i.e., 282.4 MHz), $\omega_0 = 1.77 \times 10^9$ rad/s, it is clear that $\omega_0\tau_v \gg 1$ and only $J(0)$ is significant in determining T_2 (eq 3). Thus, the contributions to the experimental line width, $\Delta\nu_{1/2}$, for vesicles from the considered motions are given by

$$\Delta\nu_{1/2}(\text{CSA}) = 1/(\pi T_2) = [4/(45\pi)]\omega_0^2\delta^2\tau_v = (16\pi/45)(\Delta\nu_{CSA})^2\tau_v \quad (6)$$

The other contribution to the line width arises from the spin–lattice relaxation (T_1), but since $T_2^{-1} \gg T_1^{-1}$ in our case, this can be ignored. The study of the motional narrowing of the line width can thus give information about the additional motions of SUV. For example, the correlation time, τ_v, can be calculated from the line widths of the SUV, $\Delta\nu_{1/2}$, and the residual CSA of multilamellar dispersions, $\Delta\nu_{CSA}$, by use of eq 6. This result can be compared to the correlation time estimated from the known particle size based on the Stokes–Einstein diffusion model (see Discussion).

For completeness, the dipolar contribution to the experimental line width (Petersen & Chan, 1977) can be estimated by the relationship:

$$\Delta\nu_{1/2}(\text{D–D}) = 1/(\pi T_2) = (4\pi/5)(\Delta\nu_{FF})^2\tau_v \quad (7)$$

From eq 6 and 7, one can see that

$$\frac{\Delta\nu_{1/2}(\text{D–D})}{\Delta\nu_{1/2}(\text{CSA})} = \frac{9}{4}\left(\frac{\Delta\nu_{FF}}{\Delta\nu_{CSA}}\right)^2 \approx 0.09 \quad (8)$$

since $\Delta\nu_{CSA} \approx 5\Delta\nu_{FF}$ (Table I). On the basis of the same argument, the dipolar contribution to other relaxation mechanisms such as T_1 and $T_{1\rho}$ will also be approximately 10% of the CSA contribution.

Off-Resonance $T_{1\rho}$ by CSA Mechanism. In all motional studies, it is desirable to extend the frequency range of motions to be investigated. Conventional NMR relaxation studies are limited to motions that can result in an observable minimum for T_1 (see eq 2). The minimum will occur at $\tau_c = 0.7/\omega_0 = 4 \times 10^{-10}$ s in our case. To determine the correlation time of relatively slow motions (10^{-6}–10^{-7} s) such as the tumbling of vesicles, spectroscopic frequencies several orders of magnitude lower would have to be used. An attractive technique to study motions of low frequency, which retains the sensitivity of a high magnetic field, is the measurement of $T_{1\rho}$, the spin–lattice relaxation in the rotating frame. [For a general review of both theoretical and experimental aspects of $T_{1\rho}$, see Ailion (1983)].

$T_{1\rho}$ caused by the anisotropy of the chemical shiift has been studied under exact resonance condition by Blicharski (1972). Unfortunately, the achievement of the $T_{1\rho}$ minimum under exact resonance condition by applying a large enough locking field, H_1, is rather difficult for correlation times in the range of 10^{-6}–10^{-7} s. Nevertheless, it has been shown by Jacquinot & Goldman (1973) that Zeeman relaxation with a small radio-frequency field applied far from resonance could yield the same kind of information as would the relaxation with a large radio-frequency field applied at resonance.

Since no explicit solution for off-resonance $T_{1\rho}$ using the chemical shift anisotropy (CSA) has been reported, a detailed formulation for the $T_{1\rho}$ due to an axially symmetric CSA tensor is given in Appendix. Explicitly, by using eq 4 for $T_{1\rho}$

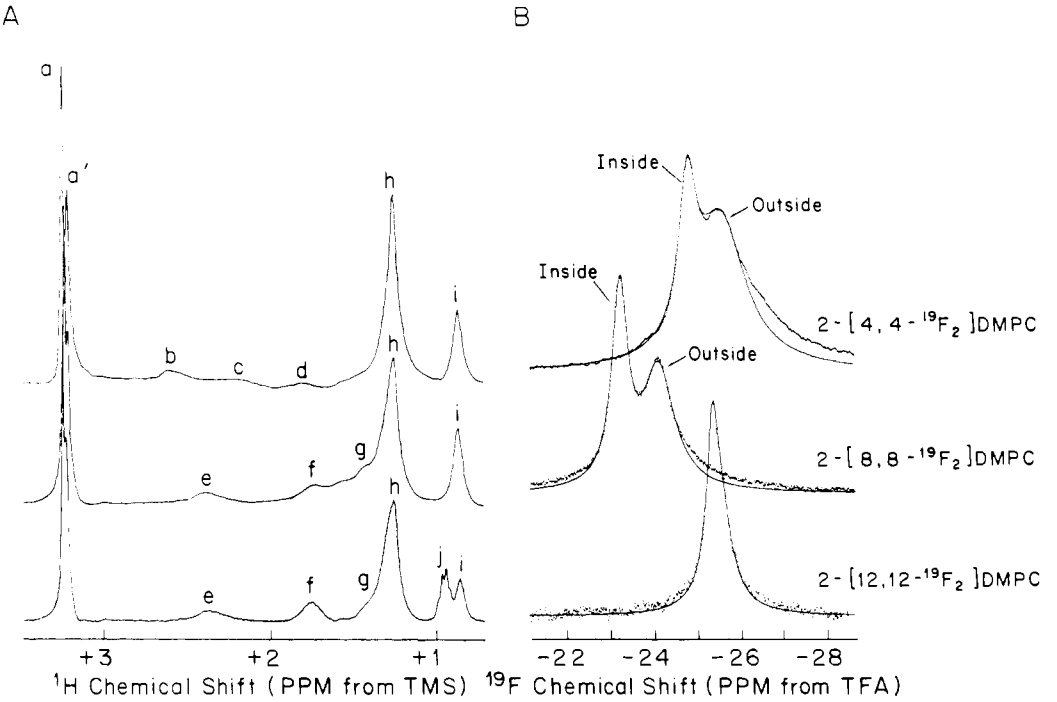

C

2-[4,4-$^{19}F_2$]-DMPC

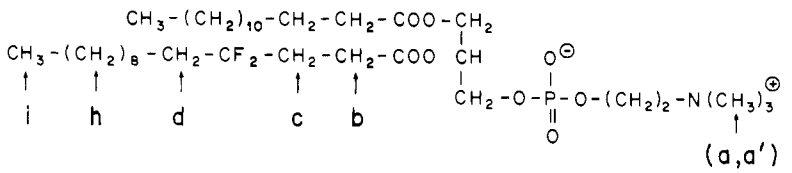

2-[8,8-$^{19}F_2$]-DMPC

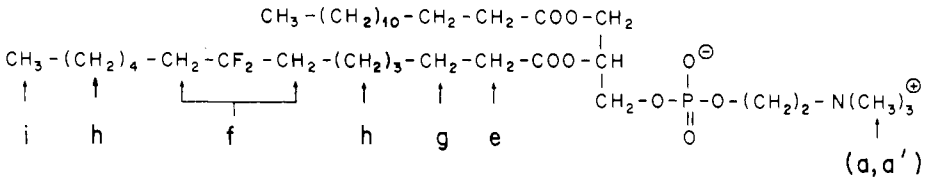

2-[12,12-$^{19}F_2$]-DMPC

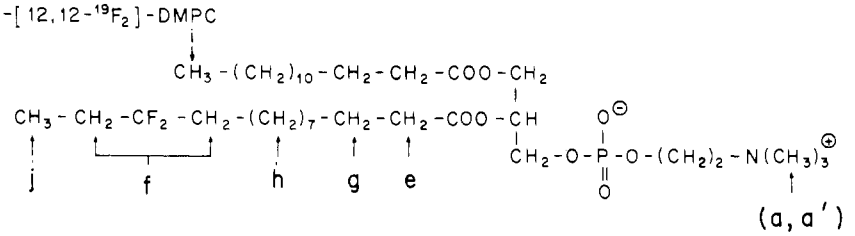

FIGURE 1: NMR spectra of ^{19}F-labeled phospholipids in sonicated unilamellar vesicles at 29 °C: (A) 300-MHz ^1H NMR; (B) 282.4-MHz ^{19}F NMR; (C) formulas for [^{19}F]DMPCs used in (A) and (B). The assignments for the various ^1H resonances are indicated by letters. The ^{19}F NMR spectra (dotted line) are fitted by a pair of Lorentzian lines to determine individual line widths and chemical shift positions.

and assuming $\omega_0 \gg \omega_e > \omega_1$ and $\omega_0\tau_c \gg 1$ in our case, a much simplified solution is obtained as

$$T_{1\rho}^{-1} = (2/45)\omega_0^2\delta^2(\sin^2\theta)[2\tau_c/(1 + \omega_e^2\tau_c^2)] \quad (9)$$

where θ is defined in eq A5 and $\omega_e = (\omega_1^2 + \Delta\omega_{off}^2)^{1/2}$. Therefore, once $T_{1\rho}$ is measured in the presence of an off-resonance frequency field, the correlation time, τ_c, can readily be calculated. Following James et al. (1977), instead of directly measuring off-resonance $T_{1\rho}$, we measure the intensity ratio between M_{eff}, the steady-state value of the magnetization component aligned with the effective field (H_e) in the presence of the off-resonance field, and M_L, the value of the magnetization component aligned with the stationary magnetic field (H_0). As suggested by Jacquinot & Goldman (1973), for a spin system with known single-exponential T_1 relaxation:

$$M_{eff}/M_L = (1 + T_1/T_{eff})^{-1} \quad (10)$$

where T_{eff} is the contribution to off-resonance $T_{1\rho}$ resulting from the off-resonance effective field. Since T_{eff} is approximated by $T_{1\rho}$ in our case [see eq 12 in James et al. (1977)], eq 9 can be combined with eq 10 to give a relationship between the measurable quantity, M_{eff}/M_L, and the correlation time, τ_c. Theoretically, one can calculate M_{eff}/M_L as a function of off-resonance frequencies, $\Delta\omega_{off}$, at a given correlation time, τ_c. The comparison between the experimental M_{eff}/M_L and the theoretical curve will then allow us to determine τ_c.

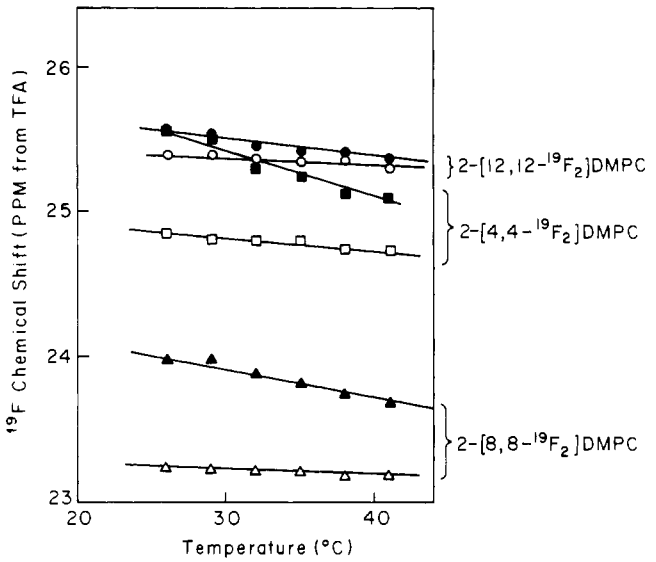

FIGURE 2: Temperature variation of the ^{19}F chemical shift for the three different ^{19}F-labeled phospholipids, as sonicated vesicles. The open symbols represent ^{19}F chemical shift positions of the inside leaflet of SUV, and solid symbols represent those of the outside leaflet: (□, ■) 2-[4,4-$^{19}F_2$]DMPC; (△, ▲) 2-[8,8-$^{19}F_2$]DMPC; (○, ●) 2-[12,12-$^{19}F_2$]DMPC.

RESULTS

Figure 1 shows both the 300-MHz ^{1}H and 282.4-MHz ^{19}F NMR spectra of SUV in 10% D_2O in the presence of 50 mM Tris, 100 mM NaCl, and 1 mM EDTA at pH 7.4. Proton resonances have been assigned (Figure 1A); note that the choline methyls (a, a′) show evidence of the bilayer structure of SUV. This is also clearly visible in the ^{19}F NMR spectra (Figure 1B), where the solid line is a simulated spectrum of two overlapping Lorentzian peaks. The assignement of the two ^{19}F NMR resonances to the inside and outside components of the SUV bilayer was confirmed by adding $MnCl_2$ to broaden the peak that is accessible to the paramagnetic Mn^{2+} ion. Our ^{19}F results (data not shown) are essentially the same as those previously reported by Longmuir & Dahlquist (1976). It should be noted that the ^{19}F resonance from the fatty acyl chain of the inside leaflet always occurs downfield relative to that of the outside leaflet, while for ^{1}H NMR, the assignment of the resonances is reversed (Schuh et al., 1982). It is also interesting to observe that the line widths from the ^{19}F NMR spectra are almost 1 order of magnitude larger than those of the ^{1}H NMR spectra (e.g., peak h in Figure 1A). Since the dipolar interaction between the fluorine pair is expected to be similar to that between the proton pair, the line width of the ^{19}F NMR spectra must be dominated by the chemical shift anisotropy at 282.4 MHz as observed by Gent et al. (1978). A similar conclusion has also been reached under Theory.

The apparent single peak of the ^{19}F NMR spectrum of 2-[12,12-$^{19}F_2$]DMPC is actually composed of two superimposed resonances. The presence of two peaks becomes clearer at lower temperatures (results not shown). For the SUV labeled at positions 4 or 8, the two resonances corresponding to the inner and outer layers are resolved at all observed temperatures (26–42 °C). The chemical shifts with respect to TFA as a function of temperature are shown in Figure 2. Apparently, the chemical shift differences between the inside and outside resonances become greater at lower temperatures. The increase of these differences, however, originates almost exclusively from the shift of the outside leaflet resonance.

Figure 3 shows the spin–lattice relaxation time, T_1, and the transverse spin–spin relaxation time, T_2^* [$=1/(\pi\Delta\nu_{1/2})$], as

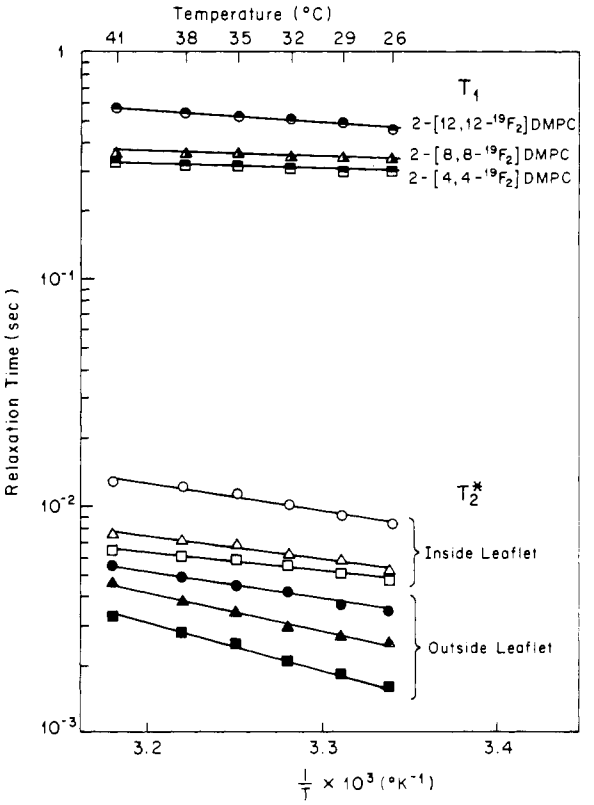

FIGURE 3: Spin–lattice relaxation times (T_1) and apparent spin–spin relaxation times [$T_2^* = 1/(\pi\Delta\nu_{1/2})$] as a function of reciprocal temperature. The open symbols represent ^{19}F relaxation data of the inside leaflet, and the solid symbols represent those of the outside leaflet: (□, ■) 2-[4,4-$^{19}F_2$]DMPC; (△, ▲) 2-[8,8-$^{19}F_2$]DMPC; (○, ●) 2-[12,12-$^{19}F_2$]DMPC. The semisolid symbols for the T_1 values indicate the same T_1 detected for the resonances from the inside and outside leaflet of SUV.

Table II: Arrhenius Activation Energy (kJ/mol) from T_1 and T_2^* for Three Different ^{19}F-Labeled Lipids in Sonicated Unilamellar Vesicles As Studied by ^{19}F NMR at 282.4 MHz: A Comparison with Values Obtained from ^{2}H and ^{1}H NMR Studies

parameters	4-position	8-position	12-position
T_1 (^{19}F NMR)	5.0	5.5	10.0
T_1^* (^{1}H NMR)[a]	6.0	6.0	11.0
T_1^* (^{2}H NMR)[b]	14.6	14.6	14.6
T_2^* (inside leaflet)	16.5	20.0	24.0
T_2^* (outside leaflet)	40.8	32.7	22.8
S_{FF}[c]	6.3	11.0	14.9

[a] See Results for the details of estimation. [b] Brown et al. (1979). [c] Post et al. (1984) determined these for multilamellar liposomes.

a function of inverse temperature for the various ^{19}F-labeled fatty acyl positions. Despite the fact that both the line widths and chemical shifts of the two resonances from the two leaflets of SUV are different, their T_1 values are the same. This result has always been assumed in previous ^{1}H, ^{2}H, and ^{13}C NMR studies (Brown et al., 1983). As in other spin–lattice relaxation measurements, ^{19}F T_1 values are larger near the end of the chain and approximately the same at the 4- and 8-positions.

The temperature dependence of the T_1 measurements shows that T_1 is larger at higher temperature, with an apparent Arrhenius activation energy of 5.0, 5.5, and 10.0 kJ/mol for the 4-, 8-, and 12-^{19}F-labeled lipids, respectively (Table II). The values for the 4- and 8-positions are lower than that for the 12-position. Since previous ^{2}H relaxation measurements (Brown et al., 1979) have not detected any dependence of the activation energy on the position in the fatty acyl chain, ^{1}H relaxation measurements on both ^{19}F-labeled and unlabeled

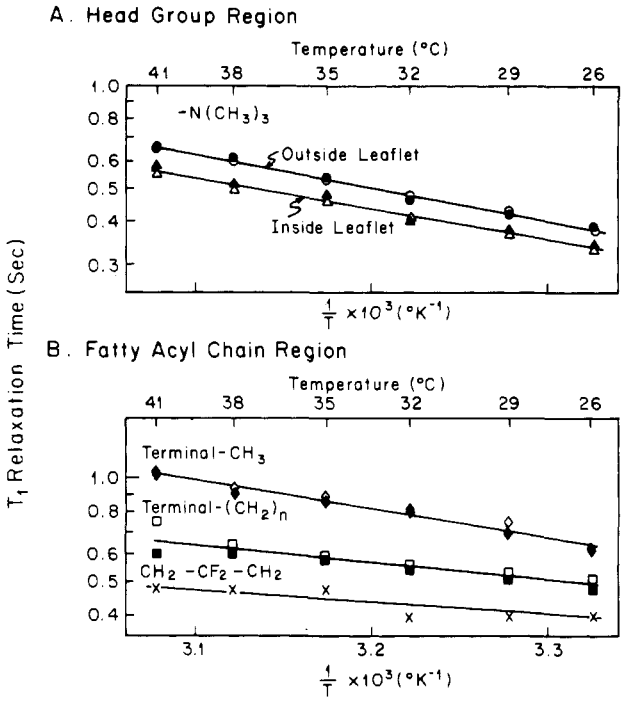

FIGURE 4: The 300-MHz ^1H T_1 measurements of DMPC and 2-[8,8-$^{19}F_2$]DMPC in sonicated vesicles as a function of reciprocal temperature. The open symbols represent ^1H relaxation data of DMPC, and the solid and cross symbols represent those of 2-[8,8-$^{19}F_2$]DMPC. (A) Head-group region; (B) fatty acyl chain region.

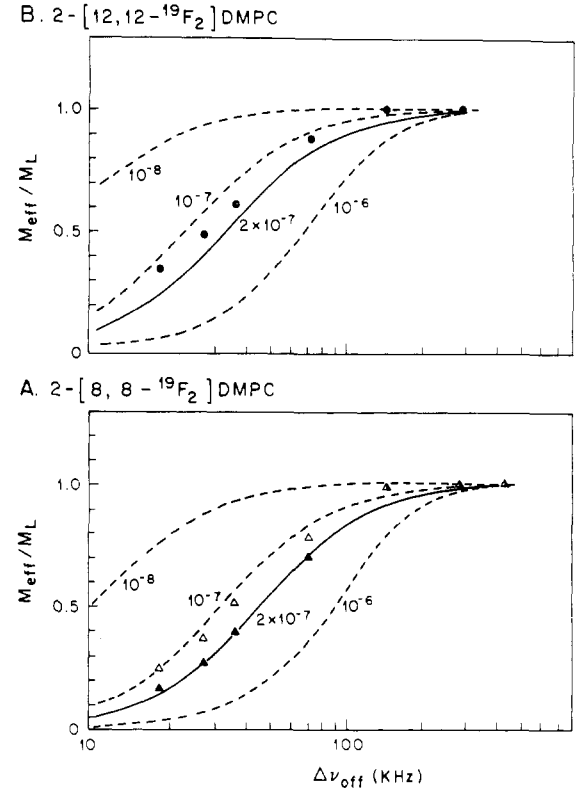

FIGURE 5: Determination of the effective correlation times by off-resonance $T_{1\rho}$ measurements at 26 °C: (A) 2-[8,8-$^{19}F_2$]DMPC; (B) 2-[12,12-$^{19}F_2$]DMPC. The theoretical curves (open and solid lines) are calculated from eq 9 and 10 by using the following parameters for various values of $\Delta\nu_{off}$ at the indicated correlation times, 10^{-6}, 10^{-7}, and 10^{-8} s: (A) $\Delta\nu_{CSA}$ = 16.9 kHz, T_1 = 0.34 s, and ω_1 = 4 kHz; (B) $\Delta\nu_{CSA}$ = 10.4 kHz, T_1 = 0.46 s, and ω_1 = 4 kHz. From a comparison of the experimental and theoretical M_{eff}/M_L values as a function of off-resonance frequency, $\Delta\nu_{off}$, the effective correlation times can be determined as 2×10^{-7} and 1×10^{-7} s for the outside and inside leaflet, respectively: (△) inside leaflet of 2-[8,8-$^{19}F_2$]DMPC; (▲) outside leaflet of 2-[8,8-$^{19}F_2$]DMPC; (●) 2-[12,12-$^{19}F_2$]DMPC, where no attempt has been made to resolve the two overlapping resonances from the inside and outside leaflets of SUV.

DMPC vesicles were performed. ^1H T_1 values are observed to be identical for these two systems (Figure 4), indicating that no perturbation of the fatty acyl packing by the CF_2 group occurs as judged from ^1H T_1 relaxation studies.

The apparent activation energy shown by T_1 measurements for the protons next to the C$^{19}F_2$ group (peak f in Figure 1) in 2-[8,8-$^{19}F_2$]DMPC vesicles has been found to be 6.0 kJ/mol. The super-Lorentzian methylene peak h (Figure 1) obtained by ^1H NMR shows T_1 values with an apparent activation energy of 11.0 kJ/mol. This value is similar to that obtained previously by Kroon et al. (1976). It should be noted that the sharp component of peak h arises mainly from the ^1H NMR signals of the terminal methylene groups (Bloom et al., 1978). Careful examination of the broad component under peak h (from the methylene groups close to the polar head group) shows a smaller activation energy (6.3 kJ/mol) of the ^1H T_1 values than that of the sharp component (from the terminal methylene groups). These results suggest that there is indeed a dependence of the activation energy on the position in the fatty acyl chain.

The T_2* values obtained by ^{19}F NMR of the SUV are, in general, 1–2 orders of magnitude shorter than those of T_1. The apparent Arrhenius activation energies derived for T_2* are, however, much larger than those from T_1 (Table II). For resonances from the inside leaflet of SUV, apparent activation energies of 16.5, 20, and 24 kJ/mol are obtained for the 4-, 8-, and 12-positions. Correspondingly, values of 40.8, 32.7, and 22.8 kJ/mol are detected for the outside leaflet of SUV. The activation energy is seen to be higher near the end of the chain for the inside leaflet, but this trend is reversed for the outside leaflet.

The results of off-resonance $T_{1\rho}$ measurements for both 2-[8,8-$^{19}F_2$]DMPC and 2-[12,12-$^{19}F_2$]DMPC in SUV are shown in Figure 5. They are compared with the theoretical curves at the indicated effective correlation time. As shown by the theoretical curves, these measurements are sensitive to the correlation time range of 10^{-6}–10^{-8} s. We should emphasize that the curves calculated for different ^{19}F-labeled lipids are different because of their different CSA values in the multilamellar dispersions (compare panels A and B of Figure 5) although their line shapes appear similar. From a simulation of the experimental data, one can conclude that the effective correlation of 2-[8,8-$^{19}F_2$]DMPC in the SUV is 2×10^{-7} and 1×10^{-7} s for the outside and inside leaflets of the bilayer at 26 °C, respectively. In the case of 2-[12,12-$^{19}F_2$]DMPC, it was impossible to resolve the inside and outside resonances at the observed temperature; still, the correlation time is similar to those obtained for 2-[8,8-$^{19}F_2$]DMPC. Interestingly, these correlation times (10^{-7} s) are almost 1 order of magnitude smaller than that expected from the reorientation of the entire vesicle on the basis of Stokes–Einstein diffusion model (10^{-6} s).

Discussion

Chemical Shift and Lateral Packing. An attempt to understand the phospholipid packing in SUV can be approached by first comparing the results of the present ^{19}F NMR study at a magnetic field of 7 T and the ^1H NMR study of SUV at a magnetic field of 11.7 T (Schuh et al., 1982). In both systems, only the broad component from the outside leaflet of SUV appears to shift, while the narrow component remains unchanged over the range of temperatures examined (Figure

2). However, the relative change and location of the two resonances from the inside and outside leaflets of SUV are reversed for the ^{19}F and ^{1}H NMR spectra. The broader resonance of the outside leaflet appears upfield relative to that of the inside leaflet in the ^{19}F NMR study, while in the ^{1}H NMR study, it is downfield. In addition, the broader peak in the ^{19}F NMR spectra is shifted upfield, while that in the ^{1}H NMR spectra is shifted downfield when the temperature is lowered.

These results can be readily understood on the basis of the well-documented mechanism of the chemical shift from ^{1}H and ^{19}F NMR studies (Emsley et al., 1966; Raynes & Raza, 1971). The present proposed mechanism for the shift observed in the ^{19}F NMR spectra is similar to that proposed by Schuh et al. (1982) for ^{1}H NMR and is different from that proposed by Longmuir & Dahlquist (1976) for ^{19}F NMR. In agreement with Schuh et al. (1982), we believe that the major forces of interactions between two lipid chains are mainly attractive and of the van der Waals type. This interaction causes expansion of the electronic cloud around the protons or fluorines in the fatty acyl region. It is well-known for ^{1}H NMR that the local paramagnetic contribution to the chemical shift is small, but it is believed to be dominant in the shielding of other nuclei such as ^{19}F. Since the nuclear shielding effects are expected to be opposite for *diamagnetic* and *paramagnetic* contributions, the same type of attractive London dispersion forces would lead to the opposite chemical shift change observed for the ^{1}H and ^{19}F NMR spectra. Hence, the study of either ^{1}H or ^{19}F NMR chemical shift should give us the same type of information on the lipid packing of SUV with the exception that the ^{19}F NMR offers a wider chemical shift range and is more sensitive to environment.

The chemical shift differences between the resonances of the inside and outside leaflets of SUV can, thus, be used as an index of the lateral packing of the phospholipids in SUV. Since the ^{19}F chemical shift of the outside leaflet is shifted upfield relative to the inside leaflet, the outer hydrocarbon chains are necessarily on the average more tightly packed than the inner chain. The same conclusion has been reached by the ^{1}H NMR study (Schuh et al., 1982) and by geometrical considerations (Huang & Mason, 1978) of the phospholipid packing in SUV. The thermal expansion coefficient of the outer monolayer must also be larger as judged from the steeper slope of its chemical shift change as a function of temperature (Figure 2). The packing differences are smaller at the 12-position than those for positions 4 and 8, as judged by the relative chemical shift difference between the inside and outside ^{19}F resonances.

T_1 and Fast Local Motion. Studies of both the temperature and frequency dependence of T_1 measurements by ^{1}H, ^{2}H, and ^{13}C NMR in lipid bilayers (Feigenson & Chan, 1974; Brown et al., 1983) have concluded that two or more characteristic correlation times must exist for the fatty acyl chain motion. In attempting to understand the details of lipid dynamics, it is generally assumed that the observed T_1^{-1} is the sum of two independent contributions as

$$T_1^{-1} = T_{1f}^{-1} + T_{1s}^{-1} \quad (11)$$

where T_{1f}^{-1} indicates the contribution from relatively fast motion and T_{1s}^{-1} is the contribution from slower motion (Brown, 1982). Although it is not clear what kind of motion will be responsible for the slower motion, it is generaly agreed that the fast motion correspond primarily to trans–gauche isomerization of the lipid acyl chain. Assuming the applicability of an isotropic model for the chain isomerization, in the short correlation time range (i.e., $\omega_0\tau_c \ll 1$), we obtain

$$T_{1f}^{-1} = (4/15)\omega_0^2\delta_0^2\tau_c \quad (12)$$

when δ_0 is the rigid lattice value for CSA. Since there is no detectable difference in T_1 for the two resonances from the inside and outside leaflets of SUV, it seems unlikely that the slow motion has a large contribution to the observed T_1 values. This interpretation of T_1 is based on the assumption of a single correlation time for the fast local motion and is a good approximation, especially at high frequencies such as 282.4 MHz used in our ^{19}F NMR measurements. Assuming that the dominant relaxation mechanism is due to local fast motion, the correlation time of this motion can be estimated from eq 12 by using a CSA value of 166 ppm (Dowd et al., 1984) and the corresponding T_1 values. The τ_c values are found to be 1.3×10^{-10}, 1.2×10^{-10}, and 0.74×10^{-10} s for the 4-, 8-, and 12-positions at 41 °C, respectively. As expected, the observed correlation time profiles in [^{19}F]DMPC show roughly a plateau for the 4- and 8-positions and a steep decrease for the 12-position. Similar results have previously been obtained by ^{2}H relaxation studies (Brown et al., 1979).

$T_{1\rho}$, T_2, and Slow Motion.* As noted under Theory, studies of $T_{1\rho}$ and of the motional narrowing of the line width should give the same kind of information about the slow motions of SUV. Using the line width ($\Delta\nu_{1/2}$) obtained from ^{19}F NMR measurements and eq 6, one should be able to calculate a correlation time. For example, the experimental line widths of 2-[8,8-$^{19}F_2$]DMPC in SUV at 26 °C are found to be 127 and 61 Hz for the outside and inside resonances, respectively. By use of the CSA value obtained for 2-[8,8-$^{19}F_2$]DMPC in multilamellar liposomes (Table I), the effective correlation times can be calculated as 3.9×10^{-7} and 1.9×10^{-7} s for the outside and inside leaflet of SUV. These values are about 2 times larger than those obtained from off-resonance $T_{1\rho}$ measurements (Figure 5). Considering our simplified approach, the agreement between $T_{1\rho}$ and T_2* data is, indeed, remarkable.

The observed corrlelation time, $(1–4) \times 10^{-7}$ s, is much smaller than that for the tumbling motion of SUV (10^{-6} s). We should emphasize here that the size distributions of our ^{19}F-labeled vesicle are very similar to those of other synthetic SUV as judged by two criteria. First, within experimental errors, the apparent line width of the ^{1}H NMR spectra for the ^{19}F-labeled lipid is the same as that obtained for DMPC vesicles. Second, the elution profile of the ^{19}F-labeled SUV from a Sepharose CL-4B column is similar to that of egg phosphatidylcholine vesicles (results not shown).

Two possible explanations can be proposed to explain the experimentally observed correlation times. The first one would be the breakdown of the Stokes–Einstein diffusion model in the case of SUV. The second one would be that we are indeed observing the slow motion proposed by Peterson & Chan (1977). Since careful hydrodynamic measurements of SUV [see Mason & Huang (1978)] have clearly demonstrated the validity of the Stokes–Einstein diffusion equation, we have to conclude that there are additional slow motions of phospholipid molecules caused by the highly curved surface of the vesicles (Bocian & Chan, 1978).

It is interesting to see that the correlation times for the two monolayers of SUV are different. Both the independent tumbling of the two uncoupled layers and the diffusion of phospholipid along surfaces of different curvature could explain the observed difference. These two motions are expected to be slow (10^{-7} s) and are consistent with the value observed in the off-resonance $T_{1\rho}$ measurements.

From the activation energies determined from T_2* measurements (Table II), information about the packing differ-

ences between the two monolayers can be obtained. According to the motional narrowing of the line width (eq 6) and assuming that the contribution of τ_c is the same for the three different ^{19}F-labeled positions, the temperature variation of the line width should correspond well to the temperature variation of the CSA in multilamellar dispersions. Since the CSA is known to correlate linearly with the order parameter (S_{FF}) (Dowd et al., 1984), one would expect that the activation energy of T_2* for SUV should also be proportional to the activation energy of S_{FF} for multilamellar dispersions. Previous work from this laboratory (Post et al., 1984) obtained an activation energy for S_{FF} of 6.3, 11.0, and 14.9 kJ/mol for the 4-, 8-, and 12-position ^{19}F-labeled lipids. Within the experimental error, these values are about half the activation energy of T_2* for the inside leaflet of SUV (16.5, 20, and 24 kJ/mol) and, therefore, indicate a similar order parameter profile in both systems. The profile of the activation energy of T_2* from the outside leaflet of SUV (40.8, 32.7, and 22.8 kJ/mol) is difficult to understand, as their trend is opposite to that of the inside leaflet. Since the chemical shift data also show significant changes in the packing of the outside leaflet, the curvature effect of SUV seems to impose perturbations mainly on the outside leaflet of the vesicles.

In conclusion, ^{19}F NMR spectroscopy with appropriate ^{19}F-labeled lipids and/or proteins offers an excellent opportunity to investigate the molecular basis of protein–lipid interactions in membrane systems. It is expected that membrane-interacting proteins or peptides will have differential effects on both the ^{19}F chemical shifts and dynamic properties of ^{19}F-labeled phospholipids in the two leaflets of membrane vesicles.

ACKNOWLEDGMENTS

We are grateful to Dr. Irving J. Lowe for discussions on both theoretical and experimental aspects of the $T_{1\rho}$ measurements, and we thank Allison K.-L. C. Lin and Dr. Ching Yao for helpful discussions on various aspects of our membrane research.

APPENDIX

Off-Resonance $T_{1\rho}$ Relaxation: Chemical Shift Anisotropy Mechanisms. In the case of axial symmetry, the anisotropic part of the chemical shielding tensor in a molecular frame can be written as

$$\sigma = \frac{2}{3}\begin{bmatrix} -(1/2)\delta & 0 & 0 \\ 0 & -(1/2)\delta & 0 \\ 0 & 0 & \delta \end{bmatrix} \quad \text{(A1)}$$

where $\delta = (\sigma_\perp - \sigma_\parallel)$. The CSA Hamiltonian of a nuclear spin I in the presence of an external magnetic field H is

$$\mathcal{H} = (\gamma\hbar)\mathbf{H}\cdot\sigma\cdot\mathbf{I} = (2/3)(\gamma\hbar\delta)[H_zI_z - (1/4) \times (H^+I^- - H^-I^+)] = (2/3)[3/(8\pi)]^{1/2}(\gamma\hbar\delta)A_{Mol}^{(0)}(\Omega) \quad \text{(A2)}$$

where Ω is the Euler angle of the molecule in laboratory frame and $A_{Mol}^{(0)}(\Omega)$ is the zeroth component of a second-order spherical tensor operator constructed with **H** and **I**. Since an irreducible tensor operator transforms under rotations as $A_{Mol}^{(0)}(\Omega) = \sum_m D_{m0}^{(2)}(\Omega)A_{Lab}^{(m)}$, where $D_{m0}^{(2)}$ are the Wigner rotation coefficients, it is possible to transform the Hamiltonian into the laboratory frame, obtaining

$$\mathcal{H} = \frac{2}{3}\left(\frac{\gamma\hbar\delta}{4\pi}\right)\left[H_0I_zF^{(0)} + \frac{6^{1/2}}{4}(H_0I^+F^{(1)} + H_0I^-F^{(-1)})\right] \quad \text{(A3)}$$

where we have chosen $H_z = H_0$, $H^+ = H^- = 0$ in the laboratory frame, and $F^{(m)}(\Omega) = (4\pi/5)^{1/2}Y_{2m}(\Omega)$ are the spherical harmonic functions.

In order to transform the Hamiltonian further into an off-resonance doubly rotating frame, we first perform an unitary transformation $U = \exp(-i\omega_0I_zt)$. Then, the coordinate system is tilted along the effective field H_{eff} and transformed again with $U = \exp(i\omega_eI'_zt)$. The resulting Hamiltonian in the doubly rotating frame can be written as

$$\mathcal{H} = \frac{2}{3}\left(\frac{\gamma\hbar\delta}{4\pi}\right)\left\{F^{(0)}H_0\left[I'_z\cos\theta - I'^{+}\frac{\sin\theta}{2^{1/2}}e^{-i\omega_et} + I'^{-}\frac{\sin\theta}{2^{1/2}}e^{i\omega_et}\right] + F^{(1)}\frac{6^{1/2}}{4}H_0\left[I'_z\frac{\sin\theta}{2^{1/2}}e^{i\omega_0t} + I'^{+}\cos^2\left(\frac{\theta}{2}\right)e^{i(\omega_0-\omega_e)t} + I'^{-}\sin^2\left(\frac{\theta}{2}\right)e^{i(\omega_0+\omega_e)t}\right] + F^{(-1)}\frac{6^{1/2}}{4}H_0\left[-I'_z\frac{\sin\theta}{2^{1/2}}e^{-i\omega_0t} + I'^{+}\sin^2\left(\frac{\theta}{2}\right)e^{-i(\omega_0+\omega_e)t} + I'^{-}\cos^2\left(\frac{\theta}{2}\right)e^{-i(\omega_0-\omega_e)t}\right]\right\} \quad \text{(A4)}$$

where θ is defined as

$$\theta = \tan^{-1}\frac{\omega_1}{\omega_0 - \omega} = \tan^{-1}\frac{\omega_1}{\Delta\omega_{off}} \quad \text{(A5)}$$

The relaxation rate is then calculated by using Abragam's master equation formalism [p 276 of Abragam (1961)]. We finally obtain

$$T_{1\rho}^{-1} = \frac{2}{45}(\gamma H_0)^2\delta^2\left[(\sin^2\theta)\frac{2\tau_c}{1+\omega_e^2\tau_c^2} + \frac{3}{2}\sin^4\left(\frac{\theta}{2}\right)\times\frac{2\tau_c}{1+(\omega_0-\omega_e)^2\tau_c^2} + \frac{3}{2}\cos^4\left(\frac{\theta}{2}\right)\frac{2\tau_c}{1+(\omega_0+\omega_e)^2\tau_c^2}\right] \quad \text{(A6)}$$

Registry No. 2-[4,4-$^{19}F_2$]DMPC, 92937-51-4; 2-[8,8-$^{19}F_2$]DMPC, 83603-94-5; 2-[12,12-$^{19}F_2$]DMPC, 92937-52-5; DMPC, 18194-24-6.

REFERENCES

Abragram, A. (1961) *Principles of Nuclear Magnetism*, pp 276, 316, Clarendon Press, Oxford.
Ailion, D. C. (1983) *Method Exp. Phys. 21*, 439–482.
Barenholz, Y., Gibbes, D., Litman, B. J., Goll, J., Thompson, T. E., & Carlson, F. D. (1977) *Biochemistry 16*, 2806–2811.
Blicharski, J. S. (1972) *Z. Naturforsch., A: Phys., Phys. Chem., Kosmophys. 27A*, 1456–1458.
Bloom, M., Burnell, E. E., Valic, M. I., & Weeks, G. (1975) *Chem. Phys. Lipids 14*, 107–112.
Bloom, M., Burnell, E. E., Mackay, A. L., Nichol, C. P., Valic, M. I., & Weeks, G. (1978) *Biochemistry 17*, 5750–5762.
Bloom, M., Davis, J. H., & McKay, A. L. (1981) *Chem. Phys. Lett. 81*, 198–202.
Bocian, D. F., & Chan, S. I. (1978) *Annu. Rev. Phys. Chem. 29*, 307–355.
Brown, M. F. (1982) *J. Chem. Phys. 77*, 1576–1599.
Brown, M. F., Seelig, J., & Haberlen, U. (1979) *J. Chem. Phys. 70*, 5045–5053.
Brown, M. F., Ribeiro, A. A., & Williams, G. D. (1983) *Proc. Natl. Acad. Sci. U.S.A. 80*, 4325–4329.
Cook, B. W., & Lowe, I. J. (1982) *J. Magn. Reson. 49*, 346–349.
Dowd, S. R., Simplaceanu, V., & Ho, C. (1984) *Biochemistry 23*, 6142–6146.

Emsley, J. W., Feeney, J., & Sutcliffe, R. H. (1966) in *High Resolution NMR Spectroscopy*, Pergamon Press, New York.
Engelsberg, M., Dowd, S. R., Simplaceanu, V., Cook, B., & Ho, C. (1982) *Biochemistry 21*, 6985–6989.
Feigenson, G. W., & Chan, S. I. (1974) *J. Am. Chem. Soc. 96*, 1312–1319.
Gent, M. P. N., Cottam, P. F., & Ho, C. (1978) *Proc. Natl. Acad. Sci. U.S.A. 75*, 630–634.
Ho, C., Dowd, S. R., & Post, J. F. M. (1985) *Curr. Top. Bioenerg. 14*, 53–95.
Huang, C. (1969) *Biochemistry 8*, 344–349.
Huang, C., & Mason, J. T. (1978) *Proc. Natl. Acad. Sci. U.S.A. 75*, 308–310.
Jacquinot, J. F., & Goldman, M. (1973) *Phys. Rev.* [*Sect.*] *B 8*, 1944–1957.
James, T. L., Matson, G. B., Kuntz, I. D., & Fisher, R. W. (1977) *J. Magn. Reson. 28*, 417–426.
Kroon, P. A., Kainosho, M., & Chan, S. I. (1976) *Biochim. Biophy. Acta 433*, 282–293.
Longmuir, K. J., & Dahlquist, F. W. (1976) *Proc. Natl. Acad. Sci. U.S.A. 73*, 2716–2718.
Mason, J. T., & Huang, C. (1978) *Ann. N.Y. Acad. Sci. 308*, 29–49.
Pace, R. J., & Chan, S. I. (1982) *J. Chem. Phys. 76*, 4228–4240.
Parmar, Y. I., Wassall, S. R., & Cushley, R. J. (1984) *J. Am. Chem. Soc. 106*, 2434–2435.
Petersen, N. O., & Chan, S. I. (1977) *Biochemistry 16*, 2657–2662.
Post, J. F. M., Cook, B. W., Dowd, S. R., Lowe, I. J., & Ho, C. (1984) *Biochemistry 23*, 6138–6141.
Raynes, W. T., & Raza, M. A. (1971) *Mol. Phys. 20*, 555–564.
Schuh, J. R., Banerjee, V., Muller, L., & Chan, S. I. (1982) *Biochim. Biophy. Acta 687*, 219–225.
Stockton, G. W., Polnaszak, C. F., Tulloch, A. P., Hasan, F., & Smith, I. C. P. (1976) *Biochemistry 15*, 954–966.
Wu, W., & Huang, C. (1981) *Lipid 16*, 820–822.

Coexistence of Simple and Mixed Bile Salt–Lecithin Micelles: An NMR Self-Diffusion Study†

P. Schurtenberger*
Laboratorium für Festkörperphysik, Eidgenössische Technische Hochschule, CH-8093 Zürich, Switzerland
B. Lindman
Physical Chemistry 1, Chemical Center, Lund University, S-221 00 Lund, Sweden
Received February 12, 1985

ABSTRACT: The aggregation behavior of bile salt and lecithin in aqueous solutions at 20 °C was studied from bile salt, lecithin, and aggregate self-diffusion coefficients obtained by means of a Fourier-transform NMR pulsed-gradient spin-echo technique. The results strongly support the coexistence of simple bile salt micelles and mixed bile salt–lecithin micelles under physiologic conditions.

In recent years, extensive investigations of the physical chemistry of model and native biliary lipid systems have been performed. In particular, the formation, size, and structure of bile salt (BS)[1]–lecithin (L) mixed micelles have been studied systematically by using various techniques such as quasi-elastic light scattering (QLS) (Mazer et al., 1980, 1984; Schurtenberger et al., 1984a,b), small-angle X-ray scattering (Müller, 1981), calorimetry (Claffey & Holzbach, 1981; Spink et al., 1982), or NMR (Stark & Roberts, 1984; Lindblom et al., 1984). Whereas the model for the structure of mixed micelles at high lecithin to bile salt molar ratios (L/BS) proposed by Mazer et al. (1980) has been widely accepted, a present controversy exists as to the precise nature of the aggregates formed at physiologic L/BS ratios (0.2–0.4) and high total lipid concentrations (C_{tot}). The model proposed by Mazer et al. (1980) suggests that simple bile salt micelles and small bile salt–lecithin mixed micelles of fixed composition coexist under these conditions. This coexistence of simple and mixed micelles was already proposed by Carey & Small (1978) and is consistent with recent cholesterol dissolution studies (Higuchi et al., 1981) and equilibrium dialysis data (Duane, 1977; Higuchi et al., 1984). However, on the basis of small-angle X-ray experiments, Müller (1981) proposed that only mixed micelles exist at physiologic L/BS ratios and that these aggregates have a structure different from those formed at higher L/BS ratios. This model was further supported by Claffey & Holzbach (1981) and Spink et al. (1982) on the basis of their calorimetry

† Supported by the Swiss National Science Foundation (Grant 3.614.80).
* Correspondence should be addressed to this author at the Department of Physics, Massachusetts Institute of Technology, Cambridge, MA 02139.

[1] Abbreviations: BS, bile salt; L, lecithin; QLS, quasi-elastic light scattering; L/BS, lecithin to bile salt molar ratio; C_{tot}, total lipid concentration; C_{BS}, bile salt concentration; C_L, lecithin concentration; FT-PGSE, Fourier-transform pulsed-gradient spin-echo; D_s, self-diffusion coefficient; D_c, collective diffusion coefficient; D_s^{BS}, self-diffusion coefficient of bile salt; D_s^L, self-diffusion coefficient of lecithin; $D_s^{Me_4Si}$, self-diffusion coefficient of Me_4Si; Me_4Si, tetramethylsilane; HMS, hexamethyldisiloxane; TC, taurocholate; TDC, taurodeoxycholate; C_{tot}^0, total lipid concentration of micellar stock solution; cmc, critical micelle concentration.

0006-2960/85/0424-7161$01.50/0